Title

A cinematographic hypothesis of cortical dynamics in perception

Permalink

https://escholarship.org/uc/item/5hp6s5nz

Journal

International Journal of Psychophysiology, 60(2)

ISSN

0167-8760

Author

Freeman, Walter J, III

Publication Date

2006-05-01

Peer reviewed

A cinematographic hypothesis of cortical dynamics in perception

Walter J Freeman
Department of Molecular & Cell Biology
University of California at Berkeley
dfreeman@berkeley.edu
http://sulcus.berkeley.edu

Abstract

The aim of this study was to measure and classify spatial patterns in sensory cortical EEGs relating to conditioned stimuli (CSs) in order to test the hypothesis, based on clinical reports, that cortical dynamics is not continuous but operates in steps that resemble frames in a cinema. Recent advances in the application of the Hilbert Transform to intracranial recordings of the EEG in animals have revealed markers for repetitive phase transitions in neocortex at frame rates in the theta band. The frames were sought in multichannel EEGs that had been recorded from 8x8 high-density arrays that were fixed on primary sensory cortices of rabbits trained to discriminate visual, auditory or somatic conditioned stimuli with reinforcement (CS+) or without (CS-). Localization of frames in EEGs was by use of a new index, $H_e(t)$, called "pragmatic information". Each spatial pattern was measured by the 64 scalar analytic amplitudes from the Hilbert transform and expressed as a 64x1 feature vector specifying a point in 64-space. Classification with respect to CS+/- was by calculation of Euclidean distances of points from centers of gravity of clusters after preprocessing by nonlinear mapping. Stable spatial patterns were found in the form of amplitude modulation (AM) of aperiodic waveforms that included all channels. The impact of a CS on a sensory neocortex reorganized background EEG into two types of sequential patterns of coordinated activity, initially local and modality-specific, later global. The initial stage of phase transitions required 3-7 ms. Large-scale cortical activity then reorganized itself repeatedly and reliably over relatively immense cortical distances within the cycle duration of the center frequency of oscillation. The size, texture, timing, and duration of the AM patterns support the hypothesis that these frames may provide the basis for multisensory percepts (Gestalts).

Key words: beta-gamma EEG oscillations, cinematographic brain dynamics, chaotic itinerancy, field theory, phase transitions, pragmatic information, spatial EEG patterns

1. Introduction

1.1. Field Theory, Phase Transitions and the Cinematographic Hypothesis

Wolfgang Köhler, a founder of Gestalt psychology through his meticulous behavioral studies in apes, came to the following conclusion: "Our present knowledge of human perception leaves no doubt as to the general form of any theory which is to do justice to such knowledge: a theory of perception must be a field theory. By this we mean that the neural functions and processes with which the perceptual facts are associated in each case are located in a continuous medium" [Köhler, 1940, p. 55]. Unfortunately, he then mistakenly identified his perceptual fields with the electrical fields of the then newly discovered electroencephalogram (EEG). Roger Sperry [1958] readily disproved this extension of his hypothesis, by placing mica strips or silver needles in the visual cortex of trained cats and monkeys and showing that the resulting distortions in electrical fields had negligible effects on behaviors involving the underlying perceptual fields. Following this demonstration, and doubtlessly because of the baffling complexity of the EEG, field theory and Gestalt theory were largely discredited among neurobiologists, who opted for network models of brain function instead of field models, and who made the action potential the central dynamical event in observing, measuring and interpreting brain function instead of the synaptic currents underlying local field potentials and the EEG.

1.2. From new Techniques to new Advances

As noted by Robert Galambos (this volume) new advances stem from new techniques; for the EEG there are two significant advances. One advance is provided by multi-channel EEG recording from arrays of closely spaced intracranial electrodes giving high spatial resolution. The spatial power spectral density (PSD_X) is calculated by over-sampling from long linear arrays, from which the spatial Nyquist sampling frequency is calculated, so that the fine textures of EEG spatial patterns can be resolved without aliasing [Freeman et al., 2000; Freeman et al., 2003b]. EEG segments often have spatial patterns with chaotic (aperiodic) carrier waves in the beta or gamma band that are spatially modulated in amplitude (AM) over the cortex [Freeman, 2005]. Each pattern in EEG signals recorded with arrays of subdural electrodes can be described by an Nx1 vector that specifies a point in N-space, where N is the number of electrodes (here N = 64). Pattern similarity for purposes of classification can be evaluated by Euclidean distances between points in N-space [Viana Di Prisco and Freeman, 1985; Barrie et al., 1996; Ohl et al., 2001].

The other advance is provided by use of the Hilbert transform to calculate the analytic phase and amplitude [Barlow, 1993; Pikovsky et al., 2001]. This decomposition of the EEG can markedly improve temporal resolution of both phase and amplitude, because the start and end points of successions of textured EEG patterns can be measured. It turns out that each AM pattern also has a pattern of phase modulation (PM) that provides a basis for defining precisely the stability of spatial coherence and synchrony [Freeman and Rogers, 2002] and for estimating the spatial extent of diameters of the domains of synchronized oscillations constituting the carrier waves [Freeman, 2003a, b].

1.2. 1. Frames, Wave Packets, and Spatial AM Patterns

These AM-PM field patterns are described as "wave packets" [Freeman, 1975/2004, 2000]. Those with carrier frequencies in the gamma band recur at rates in the high theta band; those with carrier frequencies in the beta band recur at rates in the low theta band [Freeman, 2005]. Together they provide for the possibility of describing a cinematographic mechanism [Sacks, 2004] in support of cognitive operations, by which successive frames of fields of activity form by phase transitions [Freeman, 2004b]. This mechanism incorporates the three Principles set forth by Basar [this volume] and others [e.g., Kelso, 1995; Bressler and Kelso, 2001; Tallon-Baudry, 2004]: oscillations supporting cognition, widespread coherence and long-range correlation [Vitiello, 2001], and "whole-brain work" by supersynergy as distinct from

integrative brain function. The oscillations enable Köhler's perceptual fields and Baars' [1988] "cognitive workspace". Wave packets that form by phase transitions are also candidates for Fuster's "cognits", Galambos' RFUs, Bressler's "large-scale network activity in cognition", and Bullock's new principles of organization of spikes and slow potentials [all this volume]. The basic dynamics by which they form are described by a hierarchical group theory of K-sets [Freeman, 1975/2004; Appendix 2.4 in Freeman, 2004b; Kozma et al., 2003] modeled with nonlinear differential equations [Potapov and Ali, 2001] in accord with Haken's [this volume] theory of the order parameter and slaving principle. Measurements of wave packets in the context of K-set theory provide the substance with which to specify the location, size, latency, duration, carrier frequency, and related parameters [Freeman, 2004a,b] that are required to implement field theories of brain function that are expressed both implicitly and explicitly by the reports in this volume.

The most critical evidence required for a field theory is provided by the classifiability of the AM patterns of wave packets with respect to conditioned stimuli (CSs), because this behavioral correlation affirms the cognitive significance of the patterns and validates the methods for extracting them from EEG data. The data summarized in this report were recorded from high-density arrays (inter-electrode distance = 0.79 mm) of 64 electrodes surgically fixed onto the epidural surfaces of the sensory neocortices of rabbits [Barrie et al., 1996]. Patterns were measured from the root mean square (rms) amplitudes after spatial low pass filtering, which was necessary to minimize contributions from individual electrodes, in contrast to spatial high pass filtering (Laplacians for EEG, SAM for MEG) necessary for localization. Broad temporal band pass filtering was necessary to study aperiodic carrier waves, in contrast to narrow band pass filtering commonly used to measure theta, alpha and gamma waves. The spatial AM patterns appeared in a sequence of frames after arrival of each CS that the rabbits had been trained to discriminate under classical reinforcement learning: CS+ with reinforcement and CS- without reinforcement. The method for classification of EEG patterns with respect to CSs relied on the 64x1 feature vector of rms amplitudes for each pattern to specify the location of a point in 64-space, in contrast to the techniques of PCA and ICA commonly used to isolate local EEG signals. Similar AM patterns formed clusters of points in 64-space; 2 discriminated CSs gave 3 clusters, each with its center of gravity, one for each class of CS and the third for the control background condition. Classification of an AM pattern was deemed correct when the Euclidean distance to its center of gravity was shorter than the distance to the other centers of gravity. The patterns were classified by stepwise discriminant analysis at better than chance levels with respect to CSs in rabbit data from the olfactory bulb [Viana Di Prisco and Freeman, 1985; Freeman and Grajski, 1987; Grajski and Freeman, 1989], and by Euclidean distance in data from the prepyriform, visual, auditory, and somatic cortices [Barrie et al., 1996] and the auditory cortex of the gerbil [N = 18, Ohl et al., 2001].

1.2.2. Multicortical AM Patterns, global Synchronization, and Gestalts

Intermittent high rates of classification were also found in multicortical patterns formed by EEGs from five mini-arrays fixed on the visual, auditory, somatic, entorhinal cortices and the olfactory bulb [Freeman, Gaál, and Jornten, 2003c]. The goodness of classification was reduced by removal of the data from each contributing brain area [Freeman and Burke, 2003], which demonstrated that the spatial patterns were indeed simultaneous and multicortical. Measurement of the analytic phase relations among the five areas showed that global patterns were accompanied by abrupt, transient increases in phase locking among the five areas [Freeman and Rogers, 2003]. This result by the Hilbert transform sharpened the finding by time-lagged correlation of zero-lag synchrony between pairs of cortices [Freeman, Gaál, and Jornten, 2003c] by the improved temporal resolution.

In all studies the goodness of correct classification was significant in 1 to 4 peaks of high classification rates after CS arrival. Maximal classification usually obtained in the first peak within 40-130 ms of CS onset. The reduction in strength of classification in later peaks was attributed to variation in the latencies of onset of frames in the 37-40 individual trials in each session, variation that Tallon-Baudry et al. [1996] termed 'jitter'. Only modest improvements in classification rates obtained by systematic variation of the

onset times of the samples from the sets of trials about the mean onset time across all trials [Freeman, 2003b], or by measurement of the spatial patterns of phase of the beta-gamma oscillations as markers for the location of the AM patterns related to behavior [Freeman and Barrie, 2000], indicating that the AM pattern is the primary property of the wave packet with respect to cognition, while its precise time of occurrence, duration, and carrier frequencies are secondary properties, provided that the duration is long enough to encompass at least three cycles of the main frequency [Freeman, 2003b].

1.2.3. Segmentation, Pragmatic Information, and Two Stages in Perception leading to Gestalts

The Hilbert transform is a time-domain transformation that shifts the phases of the components of a signal by $\pi/2$ radians (90°) forward for positive frequencies and backward for negative frequencies. The original signal, v_j (t), which is the EEG of the j-th channel, j = 1,64, gives the real part of a complex function, a_j (t), and the Hilbert transform of the EEG gives the imaginary part, u_j (t):

$$a_j (t) = v_j (t) + i\, u_j (t), \qquad\qquad (1)$$

where i is the square root of -1. The analytic amplitude of a_j (t) is designated by A_j (t) and is given by the square root of the sum of squares of the two parts,

$$A_j(t) = [\, v_j(t)^2 + u_j (t)^2\,]^{0.5}, \qquad\qquad (2)$$

while the analytic phase of a(t) is designated by Φ(t) and is given by the arc tangent of the ratio of the imaginary and real parts:

$$\Phi_j(t) = atan\, [u_j(t) / v_j(t)\,]. \qquad\qquad (3)$$

The Hilbert transform was used to calculate the analytic amplitude of the EEG signals, $A_j(t)$, j = 1,64 in the beta and gamma bands [Freeman, 2004a] at each digitizing step. The set of amplitudes constituted a feature vector, $\mathbf{A}^2(t)$, which served as the vectorial order parameter of the relevant cortical area. The Euclidean distance between successive points given by $\mathbf{A}^2(t)$ in 64-space, $D_e(t)$, approximated the rate of change in the order parameter. Low values marked the stability of AM patterns, whereas epochs between AM patterns gave high values of $D_e(t)$.

$$D_e(t) = \{\, 1/64\, \Sigma\, [A^2_j\, (t) - A^2_j\, (t\text{-}1)]^2\, \}^{0.5} \qquad\qquad (4)$$

The amplitude at each step in each signal, $A_j(t)$, was proportional to the density of the dendritic current under each electrode causing an IR drop across the fixed extracellular tissue specific resistance, R. The mean square of the 64 values gave $\underline{A}^2(t)$. the average power from Ohm's Law, I^2R, which served as an index of the mean rate of energy dissipated by a cortical neighborhood in sustaining the EEG.

$$\underline{A}^2(t) = 1/64\, \Sigma\, A^2_j\, (t), j = 1,64; \qquad\qquad (5)$$

The ratio of these two parameters gave a method to locate the frames despite the jitter. AM patterns were identified with high values of power and low values of change in order parameter. an index, $H_e(t)$, that Atmanspacher and Scheingraber [1990] called 'pragmatic information', $H_e(t)$ was defined at each time step as the ratio of the rate of change in dissipation of energy, as estimated by the square of the spatial instantaneous mean analytic amplitude, $\underline{A}^2(t)$, to the rate of change in the order parameter, $D_e(t)$, as estimated by the distance between successive points in 64-space:

$$H_e(t) = \underline{A}^2(t) / D_e(t) \qquad\qquad (6)$$

High values of $H_e(t)$ occurred when the analytic amplitude rose and the rate of change in the spatial AM pattern slowed, indicating an epoch with transmission at high intensity of a stable AM pattern. The hypothesis was verified that AM patterns located at peak values of $H_e(t)$ were optimally classified with respect to CSs [Freeman, 2005]. The display of AM patterns at peaks of $H_e(t)$ was facilitated by

preprocessing the data with Sammon's [1969] method for nonlinear mapping [Barrie et al., 1999]. This algorithm iteratively mapped the locations of points defined by feature vectors in 64-space into 2-space for visual display, while preserving the relative distances between the points. After mapping the points were labeled for graphic display. This technique gave unprecedented separation of AM patterns between CS+ and CS- and also the sequences of AM patterns between stimuli and responses.

1.3. Segmentation by means of the Pragmatic Information Index

Prior evidence [Freeman and Barrie, 2000; Freeman and Burke, 2003; Freeman and Rogers, 2003] suggested that from two to four epochs of high classification occurred on different trials. The present results based on group clustering indicated that varying numbers of classification-related frames occurred on individual trials, minimally two frames, and that the process of perception occurred in two stages, with differences between CS+ and CS- trials. Furthermore, the earlier phase transitions triggered by sensory input introduced frames that were localized to the primary sensory area to which the stimulus was directed, occurred with relatively short latency and duration after CS arrival, had carrier frequencies in the gamma band, and had recurrence rates in the high theta band. The later phase transitions that occurred in association with CS input had longer latency and duration, had large diameters, appeared to be multimodal, had carrier frequencies in the beta band and recurrence rates in the theta band, and appeared to occur as often in the prestimulus recording epochs. It is these later beta wave packets, with characteristics that differ from gamma wave packets [Kopell et al. 2000], that are proposed as candidates for Baars' "global work space", Basar's "whole-brain work", Bressler's [2004] "inferential constraints", Kelso's (1995) "metastable states", and Fuster's "cognits" in cognitive function involving Gestalt formation.

In summary, novel methods were used to record the EEG, to get the analytic signal, a(t), and to define from the EEG the degree of order, its rate of change, and the rate of energy dissipation in the dynamics of cortical areas. These methods provided unprecedented spatial and temporal resolution of neocortical activity patterns during acts of perception that were well controlled by classical and operant conditioning paradigms. The aim of the present report is to review briefly some of the evidence provided by these new methods, and to show how this evidence can be used to address two outstanding questions in the cerebral physiology of cognition: whether perception is based on continuous flows of neural activity or on staccato stationary patterns that are demarcated by discontinuities corresponding to first order phase transitions; and whether or not there are quantitative differences in the cognitive dynamics between the earlier and later stages of perception between the onsets of CSs and CRs.

2. Methods

The methods of electrode array assembly, surgical implantation, training, data acquisition, and preprocessing have been described [Barrie et al., 1996]. The data for each rabbit consisted of 37 to 40 trials with random alternation of CS+ and CS- presentations. Each trial lasted 6 s with onset of a CS at 3 s ending the control period and starting the test period. The 64 EEGs were analog filtered at 0.1 and 100 Hz, amplified 10K, digitized in 12 bits at 2 ms intervals, and stored in 37-40 blocks, each containing 3000x64 data points (2500x64 after temporal filtering owing to loss of 250 bins at each end of the trial blocks).

The classification of EEGs with respect to CSs was by two methods. The first method was by the nonselective Euclidean distance [Freeman and Burke, 2003]. A window of fixed duration, w_e, (32, 64, 80, 96 or 128 ms) was moved in steps equal to half the duration along the sets of 6 s trials. The temporal mean of the square of the analytic amplitude at each time step T, $A_{k,i}^2(T)$, over k = 1, w_e in the window, specified the AM pattern as a 64x1 column vector and a point in 64-space. Similar AM patterns had points close together forming a cluster. The trials were divided into even and odd numbered for training and test sets. The centers of gravity were calculated for the training set. Classification at each window time step was by calculating the distance of each point to the two centers of gravity; the classification

was 'correct' if the distance to the center of the known class was shortest. The two subsets were then reversed in cross validation. Significance was determined by the binomial probability of that number of correct classification could have happened by chance.

The classification by the second method depended on prior selection of segments by use of the index, $H_e(t)$, for pragmatic information. The mean square of the analytic amplitude over the window, w_e, after summation (equation (4)) gave an estimate for the rate of free energy dissipation. The spatial $SD_A(t)$ of $\underline{A}^2(t)$ gave the order parameter. The Euclidean distance between frames, $D_e(t)$ from the distance specified by $\mathbf{A}(t) – \mathbf{A}(t-1)$ (boldface indicating vectors), gave an estimate of the rate of change in the order parameter (equation (5)). The pragmatic information index was given by the ratio: $\underline{A}^2(t)/D_e(t)$ (equation (6)). The seven steps required for extraction of the relevant feature vectors using $H_e(t)$ and the techniques of nonlinear mapping [Sammon, 1969; Barrie et al., 1999] for preprocessing prior to multidimensional classification have been illustrated [Freeman, 2005]. Labeling after mapping gave pair wise displays of overlapping clusters of points. A line was drawn in the display plane that optimally divided the clusters, and the % correct classification was calculated. All computations were done with a MATLAB 6.5 software package [Mathworks, Inc., Natick, MA]. Further details on techniques are given in the Appendices of prior reports [Freeman, 2004a, b; 2005], including the use of classifier-directed tuning curves [Fig. 3 in Freeman et al., 2003a] to find the optimal spectral bands for spatial and temporal filtering and the three parameters required for selection of segments of $H_e(t)$: the threshold t_e for the minimal value of H_e; the optimal width, w_e, for determination of analytic amplitude squared, $\underline{A}^2(t)$; and the minimal duration, m_e, of the segment demarcated by high H_e [Freeman, 2005]. Peaks for H_e were located after setting a threshold value for t_e. A peak began when $H_e(t)$ rose above t_e and ended when it fell below t_e. The peaks that proved to be too brief to have informational value were removed by application of m_e.

In previous studies each AM pattern was accompanied by a spatial pattern of phase modulation (PM) having the form of a cone in the surface dimensions of the cortex (Freeman and Baird, 1987; Freeman and Barrie, 2000). The cone provided a basis for estimating the diameter and duration of successive cortical patterns of synchronous oscillations. Here the optimization of the parameter, w_e, served to estimate the durations of the AM patterns that were located using $H_e(t)$. An estimate of the diameters of these classified patterns was obtained by fitting a cone to their analytic phase surfaces given by $\Phi_j(t)$, j = 1,64 [Freeman, 2004b, Appendix 2.2]. The conic basis function was fitted to the analytic phase surface calculated at the time point of the maximal value of the mean $\underline{A}^2(t)$ in each epoch determined by $H_e(t)$. The slope of the cone, γ, gave the phase gradient in radians/mm. The reciprocal of the gradient gave the spatial wavelength in mm/cycle. Multiplying the wavelength by $\pi/4$ gave the diameter at half-power, $d_{0.5}$,

$$d_{0.5} = \pi /4\gamma, \qquad\qquad (7)$$

which was adopted as a measure of the soft boundary condition for the interactive cortical domain that sustained each AM pattern.

Results

3.1. Classification with respect to CS+/- Evaluated by Time-locked Stepped Window Method

The feature vectors in the collection from the window stepped across 40 trials were classified after band pass filtering at three settings: high gamma (50-80 Hz), low gamma (30-50 Hz) and beta (12-30 Hz). Very few wave packets were captured in the high gamma range, so it was dropped in further testing. Pass bands for individuals varied from the normative values after classifier-directed optimization of the filter settings with tuning curves [Freeman et al., 2003a]. The centers of gravity were calculated for the 10 CS+ trials and 10 CS- trials in the training set along with the distances from each point in the test set to the two centers. Classification was by the shorter of the two distances. The classification was 'correct' when the test point for a CS+ (or CS-) point was closest to the training center of gravity for CS+ (or CS). The training and test sets were reversed, and the calculations were repeated in cross validation.

The outcome was expressed as % correct (Fig. 1). The procedure was repeated at each window step for the duration of the 6 s trials less the 250 ms at each end lost by FIR temporal filtering. The probability that the level of 'correct classification' would occur by chance was calculated from the binomial distribution for 37-40 trials in each trial set [Barrie et al., 1996]. The results for the visual, auditory and somatosensory EEGs showed one significant peak in correct classification for segments in the gamma band within 130 ms of CS onset (Figs. 1A and B), and two later peaks for steps after filtering in the beta band (C).

3.2. Early Classification of CS+/- Feature Vectors Located by Pragmatic Information Index, H_e(t)

The hypothesis was tested that the AM patterns following CS+ arrival within the temporal epoch of 40-130 ms post-stimulus would differ from those following CS- arrival, whereas the AM patterns in the pre-stimulus epoch of –1000 to –200 ms preceding both CSs would not differ significantly. The distributions of qualifying segments for the high and low gamma pass bands are shown in Figs. 2A and B. The difference in lengths of the epochs of search was adapted to give approximately equal numbers of feature vectors in the 4 groups, owing to the sparseness of qualifying segments for gamma activity in the control period.

An example of the output of the nonlinear mapping algorithm (Fig. 3A) shows four clusters: control before CS- ( ); control before CS+ (Δ); CS- (o); and CS+(*). For each cluster in the mapping plane a center of gravity was calculated, and the SD of the cluster around that center was displayed by a circle. The pairs of clusters were graphed separately (Figs. 4B-E) for clarity. A line was drawn in the display plane between the clusters on the premise of linear separability. The % correct classification was calculated from the number of points located on the same side of the line as the center to which the points belonged, divided by the total number of points and multiplied by 100. This criterion was subject to bias in small samples, so the further requirement was imposed that the total number of feature vectors contributed by each CS had to be at least 75% of the total number of trials in the set for CS+ and CS- for the separation to be significant. The level of significance was evaluated by applying the same test to feature vectors collected in approximately equal numbers from the pre-stimulus control period.

The 4-way classification after nonlinear mapping illustrated in Fig. 3 gave the results listed in Table 1 for the four pair-wise comparisons from 3 cortices in 10 subjects. Data were available for 4 auditory cortices but only two visual cortices and three somatic cortices, so three replicates were included. A significance level of p = .01 at 73% was adopted from the distribution of classification values from the pre-stimulus period [CS+(0) vs. CS-(0)], comparable to that for the Euclidean distance method (Figs.1A and B). Significant separation was found between all post-stimulus feature vectors in epoch (0), the pre-stimulus period, and in epoch (1), the post-stimulus period: [CS+(1) vs. CS-(1) (B), CS+(1) vs. CS+(0) (C), CS-(1) vs. CS-(0) (D)] for all subjects and areas.
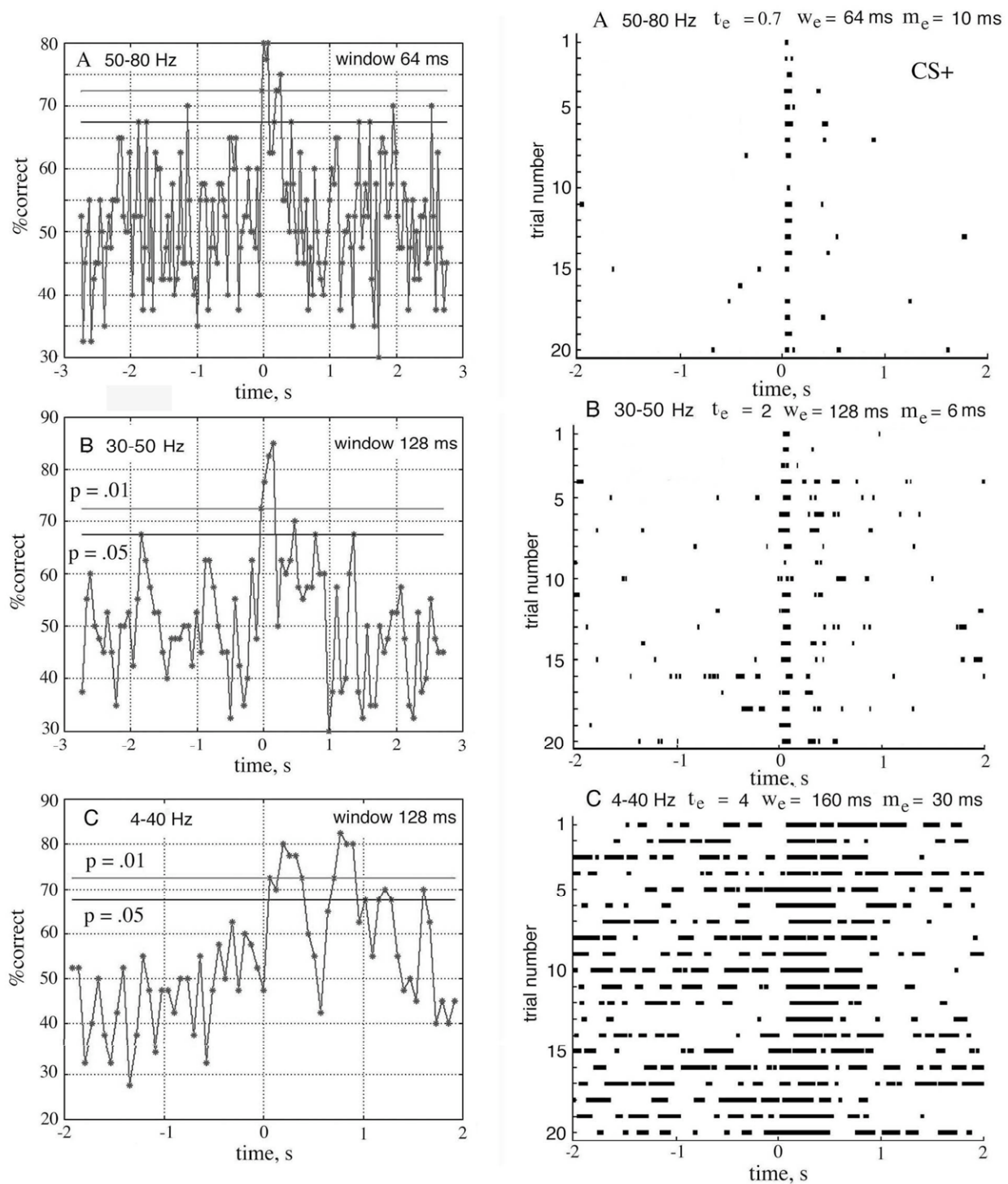
Fig. 1. Left The rates of % correct classification by the Euclidean distance method are shown for AM patterns derived from the visual cortical EEG temporally filtered in three pass bands (A-C). These kinds of curves gave optimal filter settings, estimates for epochs in which AM patterns were to be sought, and significance levels for classification. Examples from the somatic and auditory cortices showed similar features.

Fig. 2. Right The same data as those giving the curves Fig. 1 for the visual cortex gave the CS+/- epochs shown here that qualified for inclusion by the criteria established for high pragmatic information, $H_e(t)$, in three temporal pass bands (A-C). The high numbers of epochs found in the low pass band for both control and test periods suggest that the background activity that sustains the pre-stimulus state of expectancy and the post-stimulus process of decision is conducted largely in the beta band. Comparable results were found in EEGs from the somatic and auditory cortices [Freeman, 2005].
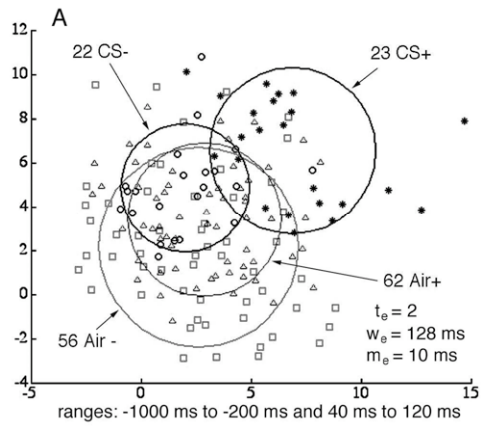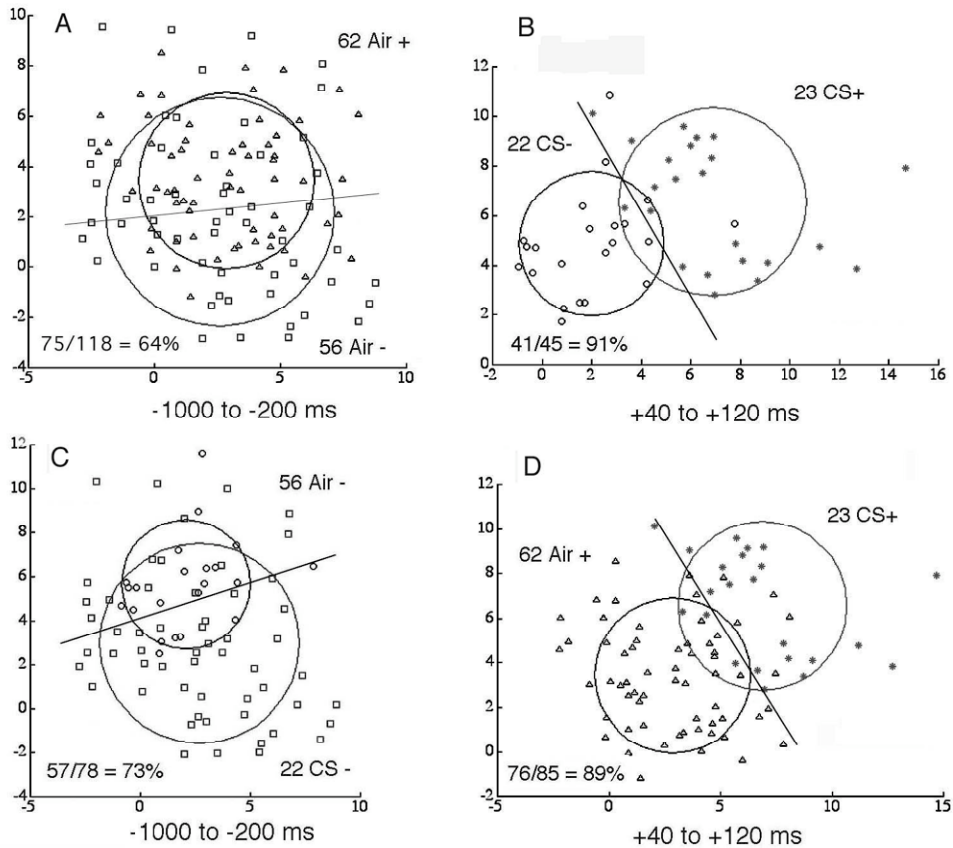
Fig. 3B-E. The % correct classification, gamma pass band, was evaluated by selectively plotting clusters in pairs and drawing a line that gave maximal separation between the two pairs of feature vectors in the display plane on the premise of linear separability. **B.** Control period: CS+ (0) vs. CS- (0). **C.** Test period: CS+ vs. CS-. **D.** Control vs. test: CS- (0) vs. CS- (1). **E.** Control vs. test: CS+(0) vs. CS+ (1).

Subsidiary aspects of the hypothesis failed in four respects. (i) The optimal frequency pass band was predicted on the basis of results from nonselective classification (Fig. 1) to occupy the upper gamma band (50-80 Hz). Four subjects conformed marginally (Table 1, marked #); the optimal pass band for the other six was broad (20-80 Hz), giving better results than restriction to the lower gamma band (20-50 Hz). (ii) The predicted optimal width of the window, w_e, for the rms of the feature vectors was the width of the peak in $H_e(t)$ given by the threshold, t_e; instead by trial and error the average optimal value for w_e was 85±27 ms. (iii) The expected minimal duration of the duration for exclusion was $m_e = 80$ ms on the basis of prior results [Barrie et al., 1996]; instead $m_e = 23±4$ ms. In these respects the apparent distributions of the information needed for classification of the feature vectors exceeded the narrow spectral, temporal, and spatial limits given by localization of the maxima in $H_e(t)$. (iv) EEGs from both subjects with a visual cortical array (Figs. 1A and B) consistently had high concentrations of epochs with high $H_e(t)$ in the early post-stimulus epoch (40-130 ms), but one of three subjects with a somatic array and three of five subjects with an auditory array (marked * in Table 1 and Table 6) did not.

Table 1. CS+ vs. CS-: pre-stimulus epoch (0) vs. first post-stimulus epoch (1): gamma band.

Epoch in ms				-1000 to –200	40-130	160-400	500-900
Subject	t_e	w_e	m_e	+0vs -0	+1vs -1	+0vs -1	+1vs -0
F152x10#	0.1	64	20	59	91	74	91
F152x12#	0.1	64	20	56	73	85	78
F9520x9#	0.1	64	12	63	87	80	80
F9520x10	2	128	12	72	87	80	83
Visual Avg	0.6	80	16	62	84	80	83
F528x2	5	128	40	55	89	89	89
L531x6*	4	64	20	62	68	83	86
F220x4#	0.5	48	14	66	85	87	78
F220x3*	9	96	10	60	69	91	84
Somatic Avg	4	84	21	61	78	88	84
F587x1	4	128	20	63	89	92	84
F553x3	2	64	10	52	78	86	91
L530x2#	0.3	64	20	59	79	83	77
L532x3*	4	64	20	69	74	82	83
F592x1*	7	64	20	64	74	83	86
Auditory Avg	4	77	18	61	79	85	84
Grand Ave	3	80	22	64	80	85	84
±SD	3	29	4	6	8	5	5

N = 40: % correct > 68%, p < .05.   % correct > 73%, p < .01.
Pass band 50-80 Hz; otherwise 20-80 Hz
*Absent alignment of epochs 40-130 ms post-stimulus (see Fig. 2)

### 3.3. Late Classification of CS+/- Feature Vectors Located by the Pragmatic Information Index, $H_e(t)$

The hypothesis was proposed on the basis of results from the time-locked stepped window method (Fig. 1) that three epochs of separable spatial patterns followed onset of the CS+ or CS- [Freeman, 2005]. The hypothesis was tested using nonlinear mapping with 6 groups: CS+ vs. CS- in epochs (40-130 ms), (160-400 ms) and (500-900 ms). Two temporal frequency pass bands were used. The upper pass band was 20-80 Hz for all cases. The lower temporal pass band was optimized for each case by calculation of tuning curves [see Fig. 3 in Freeman et al., 2003a; and Fig 2A in Freeman, 2005]. The optimal thresholds t_e and h_e and the window w_e were sought by varying each +/- an increment ~50% from an initial estimate in a 3x3x3 test set, with selection for further testing of the combination of parameters giving the best separation. Examples are shown (Fig. 2, B and C) of the distributions of qualifying segments for comparison with the results from the forced-step method (Fig. 1).

The method of AM pattern classification exemplified for the 4-group case in Fig 3 was extended to 6 groups (Figs. 4 and 5). The results from nonlinear mapping of the pair-wise classification of feature vectors in the 3 epochs are summarized in Table 2, showing significant separation of feature vectors from CS+ vs. CS- in the first epoch (40-130 ms) but not in the later epochs. Those epochs included 3 instances in which too few qualifying segments were found with which to evaluate classification. In contrast, the lower frequency pass band (averaging 7-43 Hz) gave optimal separation in epoch (500-900 ms) but less so in the earlier epochs. Those epochs also included several instances in which too few segments qualified to permit evaluation of classification (Table 3), which implied that the AM patterns being sought were scarce indeed. Comparison with Table 2 showed in all cases that classification rates in the third epoch (500-900 ms) were higher for beta pass bands than for gamma pass bands. No significant differences were noted among the three types of cortex in the later epochs, in contrast to the poor classification for the somatic and auditory cortices in the earliest epoch marked by (*) in Table 1.
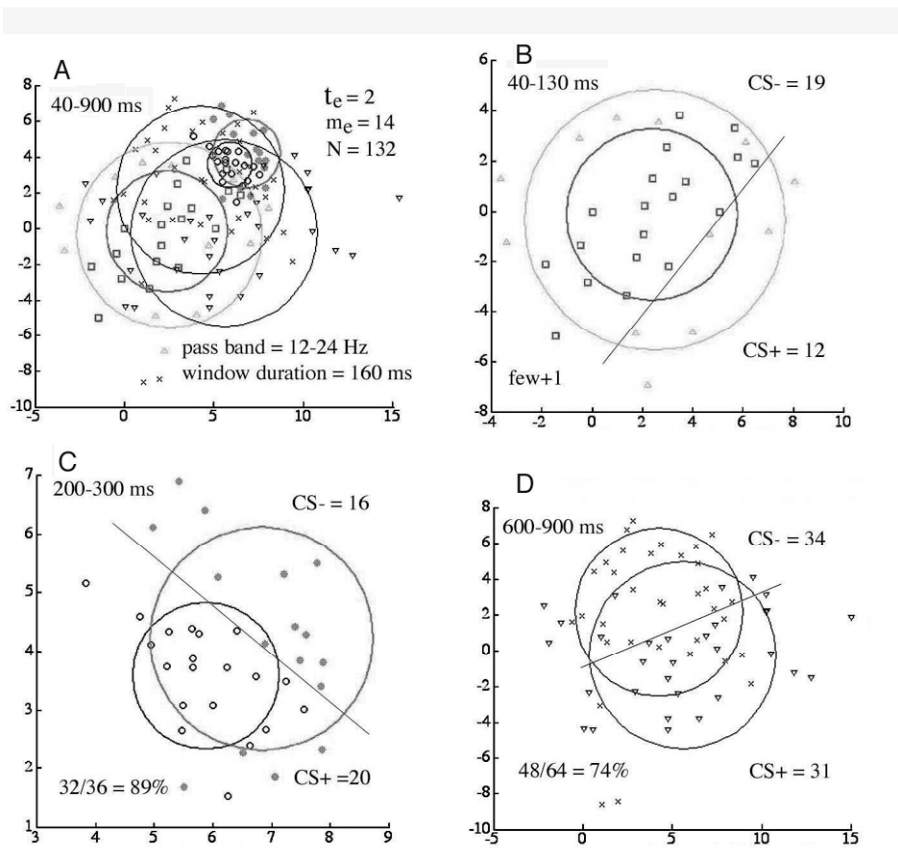
Fig. 4A. Display of 6 groups in epochs (1)-(3) from beta pass band, with breakdown by pairs of CS+/CS-. **B.** Epoch (1) (40-130 ms) **C.** Epoch (2) (200-400 ms). **D.** Epoch (3) (600-900 ms). Optimized temporal pass band = 12-24 Hz; $t_e = 2$; $w_e = 160$ ms; $m_e = 14$ ms.
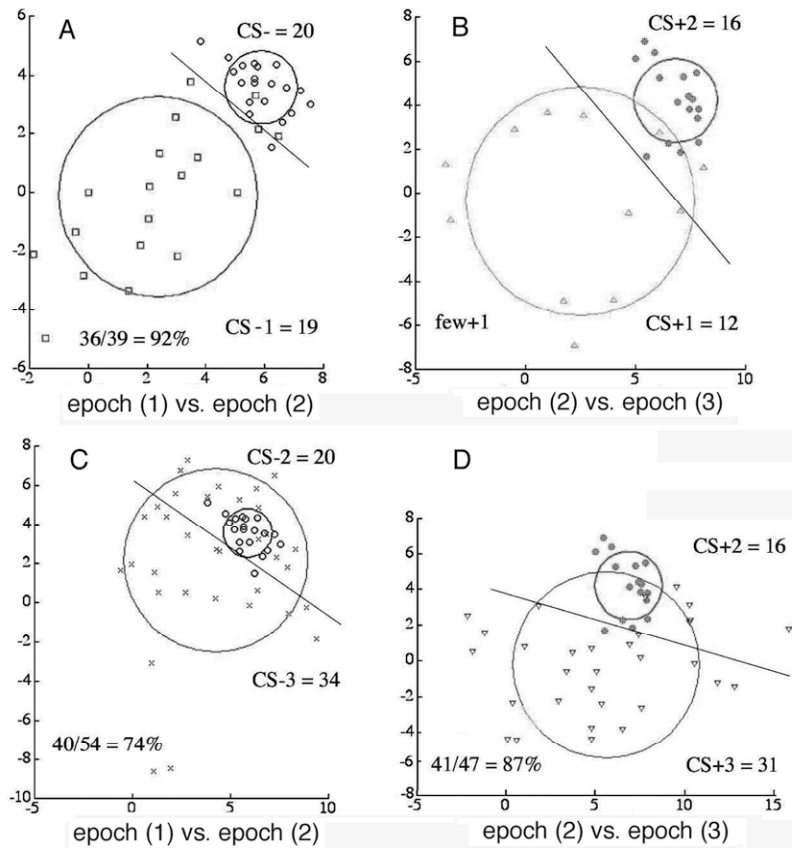
Fig. 5. The 6 groups shown superimposed in Fig. 4A are displayed in sequential pairs. **A.** CS-early vs. mid epochs with significant separation. **B.** CS+ early vs. mid epochs, separation but too few for significance. **C.** CS- mid vs. late epochs, no separation. **D.** CS+ mid vs. late epochs, separation with maximal clustering in the middle epoch (2).

Table 2. CS+ vs. CS-: Classification in three post-stimulus epochs: gamma band.

Subject	t_e	w_e	m_e	Epochs in ms 40-130 +1vs -1	160-400 +2vs -2	500-900 +3vs -3
F152x10	2	128	20	90	76	76
F152x12	2	128	20	94	74	71
F9520x9	2	128	20	85	58	59
F9520x10	2	128	6	85	77	75
Visual Avg	2	128	16	88	71	70
F528x2	5	128	20	88	84	65
L531x6	6	96	10	80	67	64
F220x4	9	96	20	82	85	57
F220x3	9	112	20	75	71	73
Somatic Avg	7	108	18	81	77	65
F587x1	3	128	10	76	62	few±3
F553x3	3	128	10	77	86	81
L530x2	5	96	10	84	75	77
L532x3	3	128	14	73	69	72
F592x1	7	128	12	87	79	57
Auditory Avg	4	122	14	79	74	72
Grand Avg	4	119	15	83	74	63
±SD	3	14	5	6	8	8

20-80 Hz: N = 40:   Correct > 68%, p < .05.   Correct > 72%, p < .01.

Table 3. CS+ vs. CS-: Classification in three post-stimulus epochs: beta band.

Subject	t_e	w_e	m_e	pass band, Hz	40-130 +1vs -1	160-400 +2vs -2	500-900 +3vs -3
F152x10	5	128	60	4-40	few±1	81	78
F152x12	2	160	14	12-24	few+1	89	75
F9520x9	4	160	16	8-56	79	79	74
F9520x10	4	160	30	4-40	few±1	84	81
Visual Avg	4	152	28	7-40	few	83	77
F528x2	13	144	20	4-56	81	few-2	77
L531x6	13	160	20	8-24	93	76	81
F220x4	10	160	20	4-56	75	76	83
F220x3	15	192	20	8-24	88	78	76
Somatic Avg	13	164	20	6-40	84	77	79
F587x1	5	192	20	16-48	61	few+2	82
F553x3	4	160	22	12-56	62	few-2	82
L530x2	11	128	26	4-56	few-1	68	79
L532x3	5	128	30	4-40	74	72	75
F592x1	15	160	30	4-24	few+1	76	76
Auditory Avg	8	160	26	8-45	66	72	79
Grand Avg	8	156	25	7-42	76	78	78
±SD	5	21	12	4-14	12	6	3

Varied frequency: N = 40.   Correct > 68%, p < .05.   Correct > 72%, p < .01.

3.4. Classification of Temporal Sequences of Feature Vectors

The nonlinear mapping method enabled comparisons between sequential pairs of spatial patterns within the CS+ and CS- trials. The same data set as that in Table 2 gave the pairs in Table 4 from the 6 groups for [CS-(1) vs. CS-(2) vs. CS-(3) and CS+(1) vs. CS+(2) vs. CS+(3)] in the epochs [40-130 ms; 160-400 ms; 500-900 ms]. Significant differences were found sequentially for the CS- feature vectors in all cases from the visual and somatic cortices and from 3 of 5 auditory cortices. Relatively few sequential pattern differences were found for CS+ feature vectors from the later epochs in the gamma frequency pass band, corresponding to the low rates of classification for CS+ vs. CS- in the later epochs (Table 2). The data set in Table 3 for the low frequency pass band gave the sequential pair-wise differences shown in Table 5. Here the CS- feature vectors in the first epoch (40-130 ms) were obscured by lack of adequate numbers for classification, whereas for CS+ the discrimination between feature vectors in the second (160- 400 ms) epoch and third (500-900 ms) epoch was more robust than that between feature vectors in the gamma pass band (Table 4).

3.5. Calculation of Properties of AM Patterns derived from Qualifying Feature Vectors

The durations of qualifying AM patterns were estimated from the optimized window durations, w_e, in Tables 1, 2 and 3. The mean duration (80±29 ms) in the first epoch (40-130 ms) was significantly less (p < .01) than that (156±21 ms) in the third epoch (500-900 ms) by paired t-test, while the mean duration (119±14 ms) in the second epoch lay between the extremes. The diameters were estimated from the half-power diameter of a right cone that was fitted by nonlinear regression to the phase surface in order to calculate the gradient of the cone [Appendix 2.2 in Freeman, 2004b] in rad/mm. Phase values were calculated from the arctangent given by the ratio of the imaginary to the real parts from equation (3) after the Hilbert transform at the time of

the peak in $\underline{A}^2(t)$ from equation (5) within the qualifying epochs of $H_e(t)$. A significant increase in mean diameter was found (Table 6, $p < .01$ by a one-tailed paired t-test) between AM patterns (21.0±9.9 mm) from in the first epoch (40-130 ms) to a mean diameter (30.0±18.1 mm) in the third epoch (500-900 ms) with the mean diameter (26.4±12.4 mm) from AM patterns in the middle epoch (160-400 ms) falling again between the extremes. Previous measurements of phase cones from AM patterns in the gamma frequency band (20-80 Hz) in these data [Freeman, 2003b] gave mean half-power diameters, $d_{0.5} = 15±3$ mm, with minimal values $d_{0.5} = 8±1$ mm and 95% inclusion $d_{0.5} = 28±7$ mm. In summary, the results showed that correctly classified AM patterns increased in size (approaching the length and hemi-circumference of the cerebral hemisphere), duration (approaching the temporal wave length of theta), and carrier wave length (approaching from above the upper limit of the alpha range) as their latencies increased from the times of onset of the CSs.

Table 4. Sequential feature vectors in 3 post-stimulus epochs: gamma band.

Epoch Subject	CS- 1st vs 2nd -1vs −2	CS- 2nd vs 3rd -2vs −3	CS+ 1st vs 2nd +1vs +2	CS+ 2nd vs 3rd +2vs +3
F152x10	98	100	78	77
F152x12	100	73	69	73
F9520x9	73	83	64	77
F9520x10	73	83	63	71
Visual Avg	86	85	68	74
F528x2	89	84	80	76
L531x6	71	68	82	74
F220x4	77	94	75	86
F220x3	90	76	56	67
Somatic Avg	82	80	73	76
F587x1	66	few-3	74	few-3
F553x4	86	62	85	76
L530x2	84	83	74	84
L532x3	69	81	75	73
F592x1	86	77	66	60
Auditory Avg	78	76	75	73
Grand Avg	82	80	72	74
±SD	11	10	8	7

Range 20-80 Hz   N = 40:   Correct ≥ 68%, p < .05   correct ≥ 72%, p < .01

Table 5. Sequential feature vectors in 3 post-stimulus epochs: beta band.

Subject	-1vs -2	-2vs -3	+1vs +2	+2vs +3
F152x10	few-1	69	few+1	91
F152x12	92	74	few+1	87
F9520x9	64	62	80	75
F9520x10	few-1	58	few+1	79
Visual Avg	few	66	few	83
F528x2	few-2	few-2	83	89
L531x6	76	86	78	79
F220x4	73	76	76	79^
F220x3	64	70	88	70
Somatic Avg	71few	77few	81	79
F587x1	63	65	few +2	76^
F553x4	few-2	few-2	80	78
L530x2	few-1	65	72	76
L532x3	86	65	63	73
F592x1	89	75	few+1	79
Auditory Avg	79few	68few	72few	76
Grand Avg	76	70	78	79
±SD	12	8	8	6

N = 40:   Correct ≥ 68%, p < .05.   Correct ≥ 72%, p < .01.

^compare range 1 vs. range 3

A further test was conducted to determine whether the information in the data that served for classification was concentrated in any smaller number than the set of 64 channels. As in prior studies [Freeman and Baird, 1987; Barrie et al., 1996; Freeman and Burke, 2003] the test was conducted by randomly deleting channels in varying numbers and repeating the classification test, while keeping an account of the contribution by each remaining channel. With one exception the results of prior studies were replicated in the present study; no channel was any more or less of value than any other, while the best classification rate was achieved by using all available channels. The exception was that in a study of the auditory cortex by Ohl, Deliano, Scheich and Freeman [2003], who found tonotopic specificity in the first classification peaks, although not in later peaks.

Table 6. Wave packet half-power diameters, $d_{0.5}$, in mm.

Subject	Early N	40-130 ms mean	±SE	Mid N	160-400 ms mean	±SE	Late N	500-1000 ms mean	±SE	Late - Early diff. mm
F152x10	39	10.5	1.4	51	12.4	1.5	54	29.0	3.3	18.5
F152x12	35	13.3	2.2	34	10.1	1.1	61	11.8	1.1	- 1.5
F9520x9	33	13.7	2.4	42	12.5	1.4	54	14.0	1.4	0.3
F9520x10	31	14.8	1.8	34	12.6	1.9	41	17.6	2.2	2.8
Visual Avg	34	13.1	2.0	40	11.9	1.5	52	18.1	2.0	5.0
F528x2	24	12.5	1.3	25	17.9	4.9	55	18.7	2.3	6.2
L531x6*	27	42.8	3.4	52	41.2	2.4	58	84.0	7.6	41.2
F220x4	34	27.3	4.0	24	36.9	3.5	162	33.8	1.8	6.5
F220x3*	36	33.0	4.9	53	39.3	4.9	62	41.9	4.4	8.9
Somatic Avg	30	28.9	3.4	38	33.8	3.9	84	44.6	4.0	15.7
F587x1	21	17.9	3.2	30	23.2	2.9	47	21.9	1.7	4.0
F553x3	24	19.1	2.1	25	16.7	2.5	51	28.7	3.3	9.6
L530x2	28	15.6	1.7	19	17.6	2.9	160	22.1	1.4	6.5
L532x3*	39	33.0	2.9	21	30.5	2.8	71	38.9	2.8	5.9
F592x1*	39	19.0	2.1	33	44.1	5.1	73	28.3	2.6	9.3
Auditory Avg	30	20.9	2.4	26	31.1	3.2	80	28.0	2.4	7.1
Grand Avg	32	21.0		33	26.4		73	30.0		9.1
±SD [±SE]	5	9.9 [2.7]		12	12.4[5.0]		40	18.6 [5.2]		10.8 [3.0]

4. Discussion

4.1. Rational for the Study of AM Patterns

There are solid reasons to focus on spatial AM patterns of EEGs from high-density arrays. Numerous unit studies in sensory and motor processing have confirmed that very many neurons cooperate in serial and parallel networks to process sensory information into percepts [Abeles, 1991; Mehring et al., 2003] and percepts into goal-directed actions [Houk, 2001; Kim et al., 2003]. Correlative studies of brain imaging by EEG, MEG, fMRI and related techniques in perception have suggested that neural signals are quickly amplified to scales of neural activity having the large sizes and long durations required to control and operate the distributed motor machinery of the brain stem, spinal cord and body. The dendritic currents that control the unit activity are the main sources of neocortical local field potentials (LFPs), EEG and MEG after extracellular smoothing by spatial ensemble averaging over thousands or millions of cortical neurons. The information necessary to identify the neural substrates of perception is expressed in the time and space dimensions of neural activity; by far the largest information capacity is in the spatial domain, whether that information is conceived to be expressed at the microscopic level in the intervals or rates of axonal pulse trains in neural networks or at the mesoscopic level in the amplitudes of LFPs generated by the dendrites. For both axonal and dendritic activities it is the relative intensities at multiple spatial locations and at various carrier frequencies that constitute the textures of spatial AM patterns.

Evidence from clinical studies reviewed by Sacks [2004] conjoined with electrophysiological data from animals [Freeman, 2004a, b] indicates that perception is "cinematographic", meaning that spatial patterns occur in discrete time steps separated by phase transitions, each with four stages: re-initialization of the phase of beta-gamma oscillations over local and also very large areas within a few ms; re-synchronization within a quarter cycle of the dominant wave length of the carrier wave; stabilization of the AM pattern (the emergence of order) with little more than the duration of a cycle at the peak carrier frequency; and a

marked increase in AM pattern intensity, all within 25-35 ms of phase reset [Freeman, 2003b, 2004a,b]. The index $H_e(t)$ for pragmatic information, which is defined as the ratio of the rate of free energy dissipation to the rate of change in the order parameter, is well suited to match the conditions postulated for maximal cortical impact on subcortical nuclei: high intensity, high synchrony, prolonged pattern stability over large coherent areas of cortex lasting 3-5 cycles of the peak carrier frequency, and a capacity for rapid discrete changes in both AM pattern and carrier frequency.

4.2. Caveats And Limitations

Use of the index $H_e(t)$ to locate pointers to AM patterns substantially improved the rates of correct classification over those achieved by the Euclidean distance method as applied across sets of CS+/- trials with fixed time steps. The new method showed that the information needed to classify the feature vectors representing AM patterns was not focal but was distributed around the $H_e(t)$ pointers over space, time and spectra. However, nonlinear mapping was an unsupervised search for optimal clustering that failed to separate 4 to 6 groups well enough so that they did not overlap. There were no statistical confidence intervals or criteria for identifying outliers and reducing their impact on the clustering. The technique used in this study of linear separation in the plane of display to define clusters had the advantage of simplicity and ease of interpretation, and it sufficed for present purposes, but there is no doubt that superior classification will accrue with application of nonlinear methods. The sensitivities of the clusters to the choice of number of groups and to varying limits on the epochs for search remain largely unexplored. Ideally the sequential clusters in each frequency band, if the appropriate number can be restricted to 2 by discriminative conditioning, should be treated as 2 multi-stage meta-patterns for each discriminated CS in the dynamic process described by Tsuda [2001] as "chaotic itinerancy"; each presentation of a CS leads to a succession of reproducible states, as suggested by the differences tabulated in Tables 4 and 5. One clear need for improvement is classification of AM patterns measured simultaneously but selectively from multiple optimized pass bands, instead of the present classification across all epochs in the same pass band. That is a formidable computational problem.

4.3. Interpretation of AM Patterns in the Perceptual Process

The salient problem in perception is how to characterize the pre-stimulus background in two aspects. One aspect concerns the repeated phase transitions that generate patterns of phase modulation in the form of cones [Freeman, 2004b]. These phase cones are associated with chaotic distributions of amplitude, and they have parameters of size and duration that conform to power law distributions. They appear to provide for the conditional stability of neocortex in a state of self-organized criticality [Freeman, 2004a], yet they have no detectable relation to specific, overt behaviors. Typically the animal subjects are motionless in prior to CS onset. The other aspect is the on-going life of each subject, in which it is to be presumed that, prior to CS arrival, each primary sensory cortex contributes to a brain state of selective attention that consists of predictions of inputs the subject expects, each with some a priori likelihood of occurrence, and that might become apparent by comparing the AM pattern sequences following CS+ (with expected action to follow) vs. CS- (no post-stimulus action is expected).

The 1/f PSDs of neocortical EEG along with the fractal distributions of the parameters of overlapping phase cones indicate that the neocortex in each cerebral hemisphere functions as a unified organ with scale-free dynamics [Freeman, 2004a]. In such a conditionally stable state each hemisphere could simultaneously generate multiple overlapping spatial AM patterns ranging in size from a few cortical columns to an entire hemisphere. Transitions at any scale require only a few ms, leading to resynchronization of beta-gamma oscillations that incorporate only a fraction of the total variance of the EEG manifesting the activity at each location. The present analysis suggests that the arrival of an expected CS+ induces formation of an AM pattern that is restricted in size to the pertinent primary sensory cortex in several or all its parts, with brief duration and a carrier frequency in the gamma band. Some 500 ms later a larger AM pattern follows that appears to include multiple sensory areas [Freeman et al., 2003c; Freeman and Burke, 2003; Freeman and Rogers, 2003], with longer duration and a carrier frequency in the beta

band. A third AM pattern may intervene with indeterminate size and frequency that may be a repetition or misclassification of either of the other two types. In simultaneous EEG recording from multiple sensory cortices the classifiable global AM patterns including all sites appear after 300 ms and not in the early post-stimulus period [Freeman and Burke, 2003]. In contrast, a known CS- also induces an early, relatively small and brief AM pattern with a carrier in the gamma band, but it is followed by a second AM pattern still with a gamma carrier frequency and a pattern that clearly differs in texture but not in size or duration. This second AM pattern may be related to response suppression rather than selection. A third AM pattern with a beta carrier, long duration, and large diameter differs from that in CS+ trials in the late epoch, perhaps only by earlier reversion to the inter-trial background state in contrast to performance of a response.

By this scenario only the early epoch has topographical information and then only if the CS provides it. The large diameter of AM patterns in cases marked by (*) in Tables 1 and 6 may have resulted from failure of the array to capture for $H_e(t)$ the putative local AM patterns in the early epoch. A likely explanation for the high failure rate for classification of early auditory AM patterns was the tonotopic restriction of the auditory CSs to 500 and 5000 Hz tones, which stood in contrast to the use of FM tones by Ohl, Scheich and Freeman [2001], to the full-field weak and stronger flashes in vision, and to the relatively broadly distributed air puff to the face or back for somesthesis. The arrays were surgically placed over the sensory areas as described in the literature for the rabbit but without topographic testing with specific CSs prior to fixation [Barrie et al., 1996]. In retrospect the more appropriate discriminanda would have been brief sounds with broad spectra such as those of a raindrop vs. a breaking twig. This scenario seems plausible, so it is offered as counterbalance to show that further analysis of EEG will require skills equally in application of techniques in neurobiology, in digital signal processing, and in multisensory perceptual conditioning.

In summary, new techniques for EEG analysis give new vistas on macroscopic brain dynamics that combine the microscopic electrophysiological properties of cortical neurons during sensory information processing and mesoscopic psychophysical properties of perception [e.g., Ricciardi and Umezawa, 1967; Pribram, 1971; Fingelkurts and Fingelkurts, 2004] and the organization of action [Houk, 2001; Kelso, 1995; Vitiello, 2001; Bressler, 2004]. This new platform can provide the foundation needed to investigate the cerebral dynamics of learning as the learning is actually taking place. "Neural activity in lightly or moderately anesthetized animals is relatively quiet, regular, and even stately. It is most suitable for the analysis of the basic topologies of connections, evaluation of fixed parameters, specification of state variables and observables, identification of intrinsic and extensive degrees of freedom, etc. In the waking animal the activity becomes more lively, especially in the presence of sensory stimuli and motivating antecedents such as food deprivation. The activity comes dramatically to the foreground when the sensory or electrical stimuli are directed into the system, from which the recordings are being made. Above all, when the animal is in a state of learning with respect to the stimulus evoking the recorded activity, that activity comes to seem cataclysmic. Great waves of potential roll off each stimulus at wildly fluctuating frequencies as immense numbers of neurons in the telencephalic masses are brought to focus on the primary cortex. Yet these waves are only the surface ripples of events within. When the full scope of the neural event in learning is eventually brought to view, it will be an awesome spectacle, even as it occurs in the brain of a mouse learning to run a maze for food. Hypotheses which express this phenomenon in terms of Pavlovian switching circuits and coincidence detectors of pulse trains may logically be correct, but their rectitude is that of the statement: 'The brain is made of neurons.' Of course that is true, but it is not the whole truth" [p. 148 in Freeman, 1972].

References

Abeles, M., 1991. Corticonics: Neural Circuits of the Cerebral Cortex. Cambridge UK: Cambridge University Press.

Atmanspacher, H., Scheingraber, H., 1990. Pragmatic information and dynamical instabilities in a multimode continuous-wave dye laser. Canadian. J. Phys., 68, 728-737.

Baars, B., 1988. A Cognitive Theory of Consciousness. Cambridge UK: Cambridge University Press.

Barlow, J.S., 1993. The Electroencephalogram: Its Patterns and Origins. Cambridge MA: MIT Press.

Barrie, J.M., Freeman W.J., Lenhart M., 1996. Modulation by discriminative training of spatial patterns of gamma EEG amplitude and phase in neocortex of rabbits. J. Neurophysiol., 76, 520- 539.

Barrie, J.M., Holcman, D., Freeman, W.J., 1999. Statistical evaluation of clusters derived by nonlinear mapping of EEG spatial patterns. J Neurosci Meth, 90, 87-95.

Bressler, S.L., 2004, Inferential constraint sets in the organization of visual expectation. Neuroinformatics 2(2), 227-238.

Bressler, S.L., Kelso, J.A.S., 2001. Cortical coordination dynamics and cognition. Trends Cog. Sci. 5, 26-36.

Fingelkurts,A.A. and Fingelkurts, A.A. Making complexity simpler: multivariability and metastability in the brain. Int. J. Neurosci. 2004, 114: 843-862.

Freeman, W.J. Waves, pulses and the theory of neural masses. Progr. Theor. Biol, 1972, 2: 87-165.

Freeman, W.J., 1975. Mass Action in the Nervous System. New York: Academic Press. Available in electronic form 2004: http://sulcus.berkeley.edu/MANSWWW/MANSWWW.html

Freeman, W.J., 2000. Neurodynamics: An Exploration of Mesoscopic Brain Dynamics. London UK: Springer-Verlag.

Freeman, W.J., 2003a. A neurobiological theory of meaning in perception. Part 1. Information and meaning in nonconvergent and nonlocal brain dynamics. Int. J. Bifurc. Chaos, 13, 2493-2511.

Freeman, W.J., 2003b. A neurobiological theory of meaning in perception. Part 2. Spatial patterns of phase in gamma EEG from primary sensory cortices reveal the properties of mesoscopic wave packets. Int. J. Bifurc. Chaos, 13, 2513-2535.

Freeman, W.J., 2004a. Origin, structure and role of background EEG activity. Part 1. Analytic amplitude. Clin. Neurophysiol., 115, 2077-2088.

Freeman, W.J., 2004b. Origin, structure and role of background EEG activity. Part 2. Analytic phase. Clin. Neurophysiol., 115, 2089-2107.

Freeman, W.J., 2005. Origin, structure and role of background EEG activity. Part 3. Neural frame classification. Clin. Neurophysiol., 116: 1117-1129.

Freeman, W.J., Baird, B., 1987. Relation of olfactory EEG to behavior: Spatial analysis: Behav. Neurosci., 101, 393-408.

Freeman, W.J., Barrie, J.M., 2000. Analysis of spatial patterns of phase in neocortical gamma EEGs in rabbit. J. Neurophysiol., 84, 1266-1278.

Freeman, W.J., Burke, B.C., 2003. A neurobiological theory of meaning in perception. Part 4. Multicortical patterns of amplitude modulation in gamma EEG. Int. J. Bifurc. Chaos, 13, 2857-2866.

Freeman, W.J., Burke, B.C., Holmes, M.D., 2003a. Aperiodic phase re-setting in scalp EEG of beta-gamma oscillations by state transitions at alpha-theta rates. Hum. Brain Mapp., 19, 248-272.

Freeman, W.J., Burke, B.C., Holmes, M.D., Vanhatalo, S., 2003b. Spatial spectra of scalp EEG and EMG from awake humans. Clin. Neurophysiol., 16, 1055-1060.

Freeman, W.J., Gaál, G., Jornten, R., 2003c. A neurobiological theory of meaning in perception. Part 3. Multiple cortical areas synchronize without loss of local autonomy. Int. J. Bifurc.

Freeman, W.J., 1987. Grajski, K.A., Relation of olfactory EEG to behavior: Factor analysis. Behav. Neurosci., 101, 766-777.

Freeman, W.J., Rogers, L.J., 2002. Fine temporal resolution of analytic phase reveals episodic synchronization by state transitions in gamma EEGs. J. Neurophysiol., 87, 937-945.

Freeman, W.J., Rogers, L.J., 2003. A neurobiological theory of meaning in perception. Part 5.

Multicortical patterns of phase modulation in gamma EEG. Int. J. Bifurc. Chaos, 13, 2867-2887.

Freeman, W.J., Rogers, L.J., Holmes, M.D., Silbergeld, D.L., 2000. Spatial spectral analysis of human electrocorticograms including the alpha and gamma bands. J. Neurosci. Meth., 95, 111-121.

Grajski, K.A., Freeman, W.J., 1989. Spatial EEG correlates of nonassociative and associative olfactory learning in rabbits. Behav Neurosci, 103, 790-804.

Houk, J.C., 2001. Frontal-subcortical circuits in psychiatry and neurology. Ch. 4 in: Lichter, D.G., Cummings, J.L. (eds.) Neurophysiology of Frontal-Subcortical Loops. New York: Guilford Publ., pp 92-113.

Kelso, J.A.S., 1995. Dynamic Patterns: The Self Organization of Brain and Behavior. Cambridge: MIT Press.

Kim, S.P., Sanchez, J.C., Erdogmus, D., Rao, Y.N., Wessberg, J., Principe, J.C., Nicolelis, M., 2003. Divide-and- conquer approach for brain machine interfaces: nonlinear mixture of competitive linear models. Neural Networks, 16, 865-871.

Kopell N, Ermentrout GB, Whittington MA, Traub RD. Gamma rhythms and beta rhythms have different synchronization properties. Proc., Nat. Acad. Sci. 97, 2000, 1867-1872.

Kozma, R., Freeman, W.J., Erdí, P., 2003. The KIV model – nonlinear spatio-temporal dynamics of the primordial vertebrate forebrain. Neurocomputing, 52, 819-826.

Mehring, C., Hehl, U., Kubo, M., Diesmann, M., Aertsen, A., 2003. Activity dynamics and propagation of syncrhonus spiking in locally connected random networks. Biol Cybern, 395-408.

Köhler, W., 1940. Dynamics in Psychology. New York, Grove Press.

Ohl, F.W., Scheich, H., Freeman, W.J., 2001. Change in pattern of ongoing cortical activity with auditory category learning. Nature, 412, 733-736.

Ohl, F.W., Deliano, M., Scheich, H., Freeman, W.J., 2003. Early and late patterns of stimulus-related activity in auditory cortex of trained animals. Biol. Cybern., 88, 374-379.

Pikovsky, A., Rosenblum, M., Kurths, J., 2001. Synchronization - A Universal Concept in Non-linear Sciences. Cambridge UK: Cambridge UP.

Potapov, A.B., Ali, M.K., 2001. Nonlinear dynamics and chaos in information processing neural networks. Diff Eq Dynamical Systems, 9, 259-319.

Pribram, K.H. Languages of the Brain. Engelwood Cliffs NJ: Prentice-Hall, 1971.

Ricciardi, L.M. and Umezawa, H., 1967. Brain and physics of many-body problems, Kybernetik 4, 44-48.

Sacks, O., 2004. In the river of consciousness. New York Review, 51, Number 1, January 15.

Sammon, J.W., 1969. A nonlinear mapping for data structure analysis. IEEE Trans. Comput. C-18, 401-409.

Sperry, R.W., 1958. Physiological plasticity and brain circuit theory. In: Harry F. Harlow & Clinton N. Woolsey (eds.) Biological and Biochemical Bases of Behavior. Madison, Univ. Wisconsin, pp 401-424.

Tallon-Baudry, C., Bertrand, O., Delpuech, C., Pernier, J., 1996. Stimulus-specificity of phase-locked and non phase-locked 40-Hz visual responses in human. J. Neurosci., 16, 4240-4249.

Tallon-Baudry, C., 2004. Attention and awareness in synchrony. Trends Cognit Sci, 8, 523-525.

Tsuda, I., 2001. Toward an interpretation of dynamics neural activity in terms of chaotic dynamical systems. Behav. Brain Sci., 24, 793-847.

Viana, Di Prisco, Freeman, W.J., 1985. Odor-related bulbar EEG spatial pattern analysis during appetitive conditioning in rabbits. Behav Neurosci, 99, 964-978.

Vitiello, G., 2001. My Double Unveiled. Amsterdam: John Benjamins.